AGU ADVANCING EARTH AND SPACE SCIENCE

Geophysical Research Letters

RESEARCH LETTER
10.1029/2020GL089343

Tropospheric Forcing of the 2019 Antarctic Sudden Stratospheric Warming

Xiaocen Shen[1,2], Lin Wang[1,2], and Scott Osprey[3,4]

[1]Center for Monsoon System Research, Institute of Atmospheric Physics, Chinese Academy of Sciences, Beijing, China, [2]College of Earth and Planetary Sciences, University of Chinese Academy of Sciences, Beijing, China, [3]Atmospheric, Oceanic and Planetary Physics, University of Oxford, Oxford, UK, [4]National Centre for Atmospheric Science, University of Oxford, Oxford, UK

Key Points:
- Both the linear and nonlinear contributions of anomalous wavenumber 1 led to the Antarctic sudden stratospheric warming in September 2019
- The wave source of this unusual wave activity can be traced back to persistent anomalous convection over the South Pacific
- The easterly phase of the quasi-biennial oscillation in the upper stratosphere sets a favorable mean state

Supporting Information:
- Supporting Information S1

Correspondence to:
L. Wang,
wanglin@mail.iap.ac.cn

Citation:
Shen, X., Wang, L., & Osprey, S. (2020). Tropospheric forcing of the 2019 Antarctic sudden stratospheric warming. *Geophysical Research Letters*, *47*, e2020GL089343. https://doi.org/10.1029/2020GL089343

Received 18 FEB 2020
Accepted 16 SEP 2020
Accepted article online 28 SEP 2020

Abstract The strongest and most persistent upward propagation of zonal wavenumber 1 (WN1) Rossby waves from the troposphere on record led to the rare Antarctic sudden stratospheric warming (SSW) in September 2019. The dynamical contribution from instantaneous anomalous WN1 and its linear interference with the climatological WN1 contributed equally to the event. The unprecedented WN1 planetary wave behavior is further attributed to a long-lived midlatitude circumpolar Rossby wave train in the troposphere that was sustained by anomalous convection, first over the subtropical Pacific Ocean east of Australia and then over the eastern South Pacific. Besides the tropospheric wave forcing, the phase of the quasi-biennial oscillation in the upper stratosphere also facilitated the weakening of polar vortex. Moreover, this SSW strongly influenced the tropospheric circulation via the Southern annular mode, favoring conditions linked to the 2019 bushfires in eastern Australia.

Plain Language Summary A sudden stratospheric warming (SSW) is an extreme event associated with rapid warming high up in the stratosphere, which can influence weather conditions at the surface. In September 2019, a rare strong SSW occurred in the Southern Hemisphere, providing further insight into these events. Here, we show that this SSW was caused by exceptionally strong and long-lasting atmospheric waves propagating upward from the troposphere into the stratosphere. Anomalous tropical convection is a possible source for these large-scale atmospheric waves. Besides, the zonal winds in the tropical upper stratosphere set a favorable background condition for the occurrence of the SSW. Our results also link the SSW to subsequent anomalous tropospheric circulation and the late 2019 bushfires in eastern Australia.

1. Introduction

The polar stratosphere was very unusual in 2019–2020 (Hu, 2020). A strong sudden stratospheric warming (SSW) occurred in the Southern Hemisphere in September 2019 (Shen et al., 2020; Yamazaki et al., 2020; also see Figure S1 in the supporting information). The SSW featured the strongest polar-cap warming and the second strongest circumpolar westerly jet deceleration from 1979 to the present (Shen et al., 2020). Though classified as minor, in that the 10-hPa 60°S zonal mean zonal wind was not easterly at any point, the SSW is accompanied by the smallest Antarctic ozone hole on record (WMO, 2019), breaking the record set by the only Antarctic major SSW in 2002 (e.g., Baldwin et al., 2003; Newman & Nash, 2005). Due to its rarity and potential links with anomalous tropospheric circulation, we are motivated to identify those unique conditions linked to the event.

The occurrence of SSWs can be well explained by planetary wave forcing originating from the troposphere (Andrews et al., 1987; Matsuno, 1971). Although planetary waves are usually weaker in the Southern Hemisphere as compared with the Northern Hemisphere due to comparatively weak land-sea thermal contrasts and smaller orography (e.g., Waugh & Polvani, 2010), they may occasionally amplify via atmospheric blocking, specific circulation patterns, or other atmospheric external forcing (e.g., Nie et al., 2013; Nishii et al., 2009; Nishii & Nakamura, 2004; Shen et al., 2020; Xiao et al., 2016). As a result, the upward propagation of planetary waves into the stratosphere can be enhanced via the linear interference between anomalous and climatological planetary waves, and the nonlinear instantaneous contributions from anomalous planetary waves (Nishii et al., 2009; Smith & Kushner, 2012). Although the planetary wave forcing in the

2019 Antarctic SSW was weaker than that in the 2002 major Antarctic SSW regarding its peak, it was the most persistent on record (Shen et al., 2020). Nevertheless, it remains unclear how the long-lived planetary wave forcing was formed, and this issue will be addressed in this study.

2. Data and Method

The four-times-daily reanalysis data used here are from the Japanese 55-year (JRA-55) reanalysis dataset (Kobayashi et al., 2015), which has a 1.25° × 1.25° horizontal resolution and extends from 1,000 to 1 hPa with 37 layers. These data are further averaged into daily means and compared against interpolated daily mean outgoing longwave radiation (OLR) data from the National Oceanic and Atmospheric Administration. The OLR data have a 2.5° × 2.5° horizontal resolution and are used as a proxy for tropical convection (Liebmann & Smith, 1996). Only data after 1979 are used due to the scarceness of Southern Hemisphere observations at high latitudes before this time. A daily climatology is defined as the value of a particular calendar day averaged over the 40-year period 1979–2018, and the daily anomaly is defined as the departure from this daily climatology. The three-dimensional Plumb flux (Plumb, 1985) and the zonal mean Eliassen-Palm (EP) flux (Andrews et al., 1987) are employed to illustrate the horizontal and vertical propagation of quasi-stationary waves. Fourier transformation is used to derive components with different zonal wavenumbers (WNs). The southern annular mode (SAM) patterns are defined as the leading empirical orthogonal function (EOF) of the September–December mean geopotential height anomalies south of 20°S at 37 pressure levels during 1979–2018 (Thompson et al., 2005). The daily SAM index is generated by projecting the daily geopotential height anomalies at 37 pressure levels onto the respective SAM patterns. The 45°S to 75°S averaged zonal mean eddy heat flux ($[v^*T^*]$) across 100 hPa is used to denote the planetary wave energy entering the stratosphere (e.g., Polvani & Waugh, 2004). Here, v and T denote the meridional wind velocity and air temperature, respectively, and the squared bracket and asterisk indicate the zonal mean and the deviation from the zonal mean, respectively. The anomalous $[v^*T^*]$ can be further decomposed into two parts $[v^*T^*]_a = [v_c^*T_a^* + v_a^*T_c^*] + [v_a^*T_a^*]_a$ (Nishii et al., 2009, 2011), where the subscripts c and a denote the climatology and anomaly, respectively. The first and second terms on the right-hand side indicate the linear interference between the climatological planetary wave and the anomalous Rossby wave packet/train, and the third term represents the instantaneous contribution from the anomalous Rossby wave packet/train.

3. Results

The peak planetary wave forcing in the 2019 Antarctic SSW was weaker than that in the 2002 Antarctic SSW (Shen et al., 2020), but the two SSWs occurred on different calendar days. To highlight how exceptional the planetary wave forcing in 2019 was compared with the climatology, Figure 1 shows the evolution of the normalized 45°S to 75°S averaged zonal mean eddy heat flux across 100 hPa, where the standard deviation (σ) derived from 1979–2018 on each calendar day was used in the normalization. Persistent and long-lasting eddy heat flux occurred before the peak of the 2019 SSW with the maximum exceeding -6σ (Figure 1a). This unprecedented eddy heat flux is the strongest over the analysis period (1979 to 2019), not only on the respective calendar day but also during the whole period from August to September. Heat fluxes even exceed those of the 2002 major SSW, which were the strongest concerning the non-standardized values and much shorter lived (Shen et al., 2020). Further decomposition suggests that the eddy heat flux causing this SSW is dominated by WN1 (Figures 1b–1d) that persisted for approximately 1 month and exceeded -10σ during its maximum, the strongest and most long-lasting during our analysis period with respect to the calendar day (Figure 1b). Previous studies suggest that the persistence of eddy heat flux is more important for decelerating the zonal mean zonal winds than the strength of the eddy heat flux pulses themselves (Polvani & Waugh, 2004; Sjoberg & Birner, 2012). Thus, it is believed that both the exceptional persistence and strength of WN1 were crucial to the formation of this 2019 minor SSW. In contrast, the eddy heat flux before the peak of the 2002 SSW had contributions from WN1, WN2, and WN3, all of which exceeded -3σ (Figures 1b–1d).

The exceptional behavior of WN1 during the 2019 SSW motivates an investigation of its evolution and origin in more detail. Figure 2 shows the pentad (5 days) mean EP flux anomalies of WN1, which are scaled by the climatological standard deviation at each pressure level (de la Cámara et al., 2019; White et al., 2019), and their divergences from mid-August to mid-September 2019. Enhanced upward propagation of WN1 from

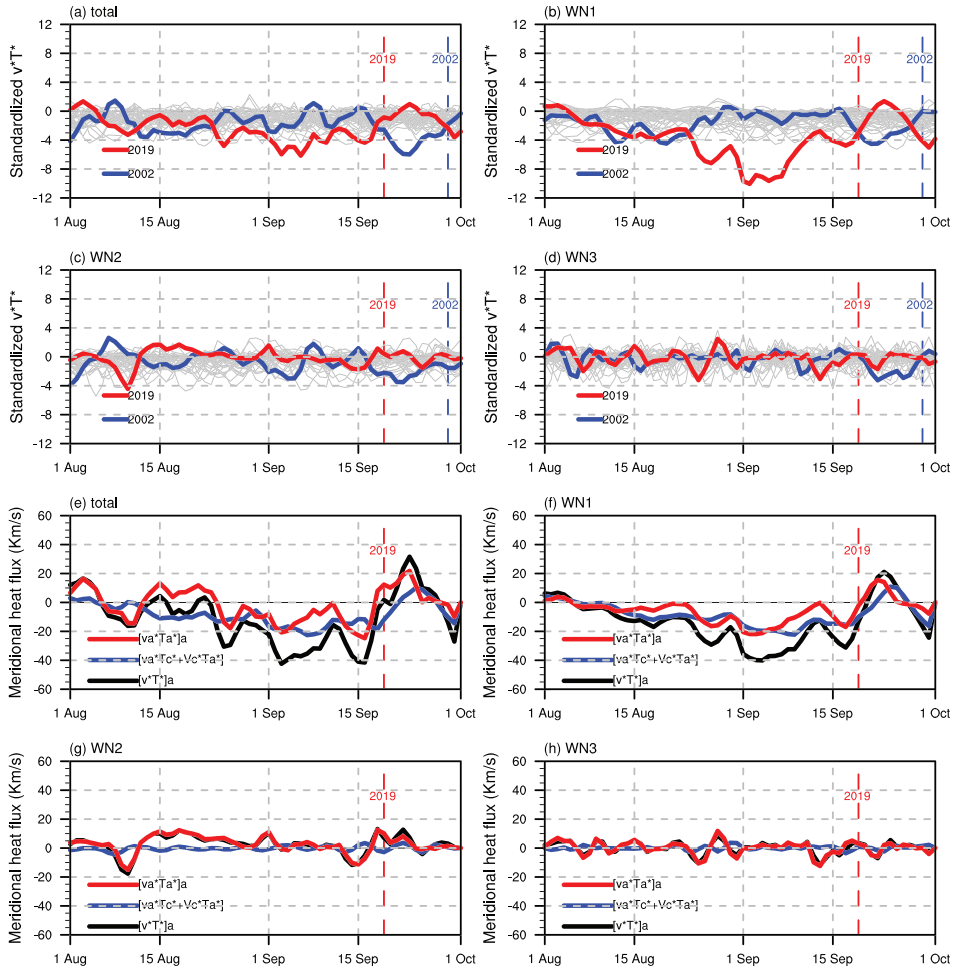

Figure 1. (a) Daily evolution of the normalized 45°S to 75°S averaged zonal mean eddy heat flux at 100 hPa from 1 August to 1 October in 2019 (red), 2002 (blue), years from 1979 to 2018 except 2002 (gray). Red and blue vertical dashed lines indicate 19 September 2019 and 29 September 2002, respectively, the date when the maximum warming was observed (Figure S1). (b–d) The same as (a) but for WN1, WN2, and WN3 components, respectively. (e) The daily evolution of the 45°S to 75°S averaged zonal mean eddy heat flux anomalies at 100 hPa in 2019. Black, blue, and red lines indicate the total anomaly, the interference term, and the instantaneous contribution, respectively. Red dashed vertical line indicates 19 September. (f–h) The same as (e) but for WN1, WN2, and WN3 components, respectively.

the troposphere into the stratosphere persisted for about 1 month around 60°S. The resultant anomalous convergence of EP flux in the middle and upper stratosphere decelerated the circumpolar westerly (Figure 2) and resulted in the stratospheric polar warming (Figure S1). These results are consistent with Figure 1 and the mechanism of SSWs (Andrews et al., 1987).

To better understand how the enhanced upward propagation of WN1 formed, the pentad mean 250-hPa geopotential height anomalies were analyzed (Figure 3). A circumpolar Rossby wave train was observed in the middle latitudes from mid-August to mid-September (Figure 3). The crests and troughs of this Rossby wave train projected well onto the anomalous WN1 component (Figure S2) and contributed substantially to the amplification of WN1. The development of this Rossby wave train formed a persistent blocking system near South America since mid-August, which is suggested to amplify the climatological ridge thus enhancing the upward propagation of planetary waves (Shen et al., 2020). However, closer inspection indicates that this linear interference between the anomalous and climatological WN1 (i.e., $[v_c{}^*T_a{}^* + v_a{}^*T_c{}^*]$) only explained approximately half of the eddy heat flux of WN1 before the SSW (Figures 1f and S3), the instantaneous contribution of the anomalous WN1 (i.e., $[v_a{}^*T_a{}^*]_a$) explained the other half from 20 August onward (Figure 1f). Those results indicate that the circumpolar Rossby wave train in Figure 3 was responsible for

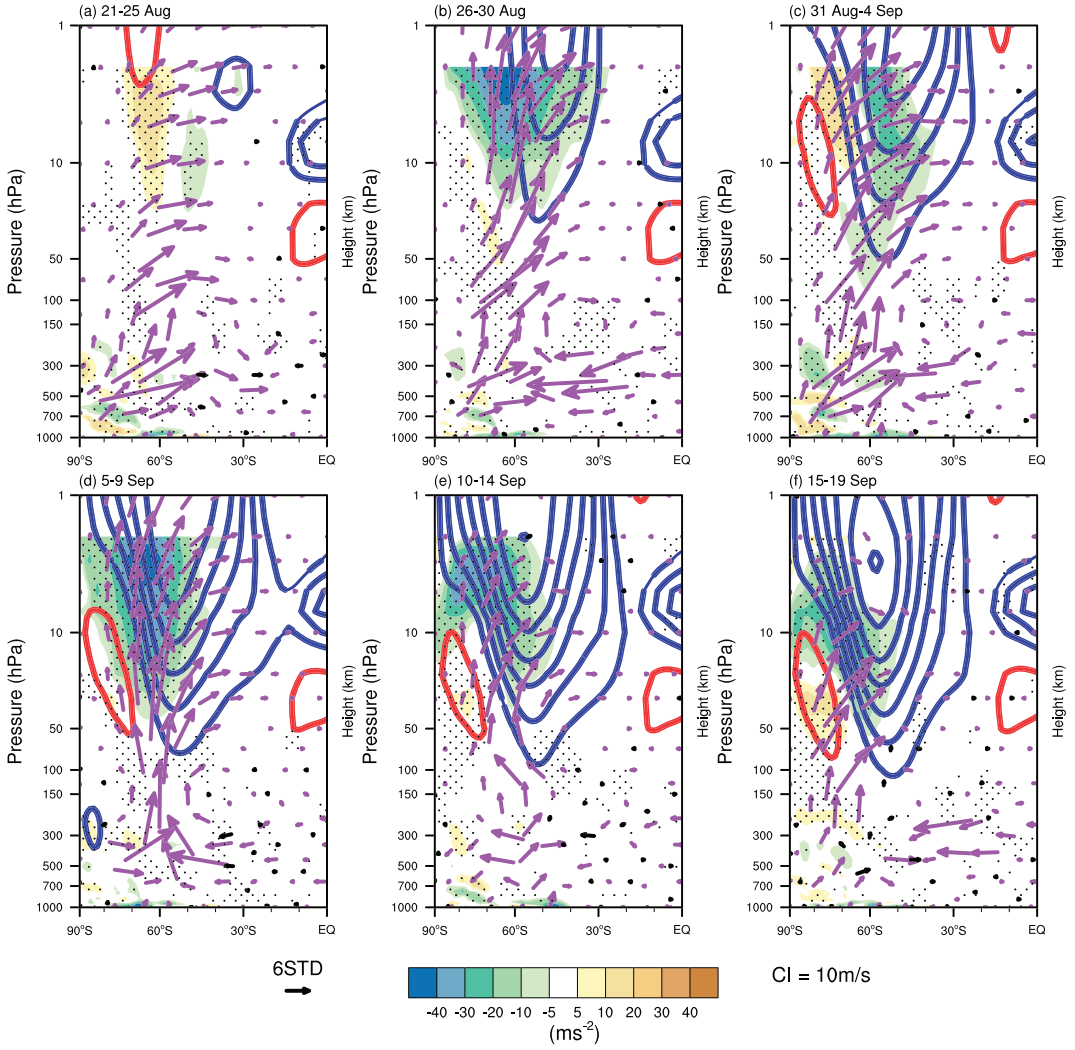

Figure 2. Five-day averaged anomalies of the EP flux of WN1 (vector), convergence of the EP flux of WN1 (shading, SI = 20 m/s^2), and zonal mean zonal wind (contour, CI = 10 m/s) during (a) 21–25 August, (b) 26–30 August, (c) 31 August to 4 September, (d) 5–9 September, (e) 10–14 September, and (f) 15–19 September in 2019. Values exceeding the 99% or 1% percentile estimated from 1,000 bootstrapped samples on each calendar day during 1979–2018 are marked as purple vectors for the EP flux, black dots for the EP flux convergence, and thick contours for zonal winds. Zero contours are omitted. Red and blue contours denote positive and negative values, respectively.

the abnormal WN1 activity during the 2019 SSW and contributed via both the linear constructive interference and nonlinear processes. WN2 and WN3 also contributed to the enhanced eddy heat flux around 15 September (Figures 1g and 1h), but their overall contributions are negligible compared with that of WN1.

The midlatitude circumpolar Rossby wave train was very persistent before the SSW, transferring energy downstream (Figure 3). It is the persistence of this Rossby wave train that explains the persistence of the total and WN1 eddy heat flux (Figures 1a, 1b, 1e, and 1f). Further inspection suggests that this Rossby wave train emanated from the subtropical Pacific Ocean east of Australia at the end of August and in early September (e.g., Figures 3b and 3c), and resembled the Pacific-South America (PSA) pattern (Mo & Higgins, 1998). Enhanced convection (reduced OLR) can be found to the east of Australia during this time (Figures 3b and 3c). The associated latent heat release and the resultant upper-tropospheric divergence (Figures S4b and S4c) could serve as the Rossby wave source (Sardeshmukh & Hoskins, 1988), which sustained and even amplified (e.g., Figure 3c) the Rossby wave train before 5 September. After 5 September, the Rossby wave

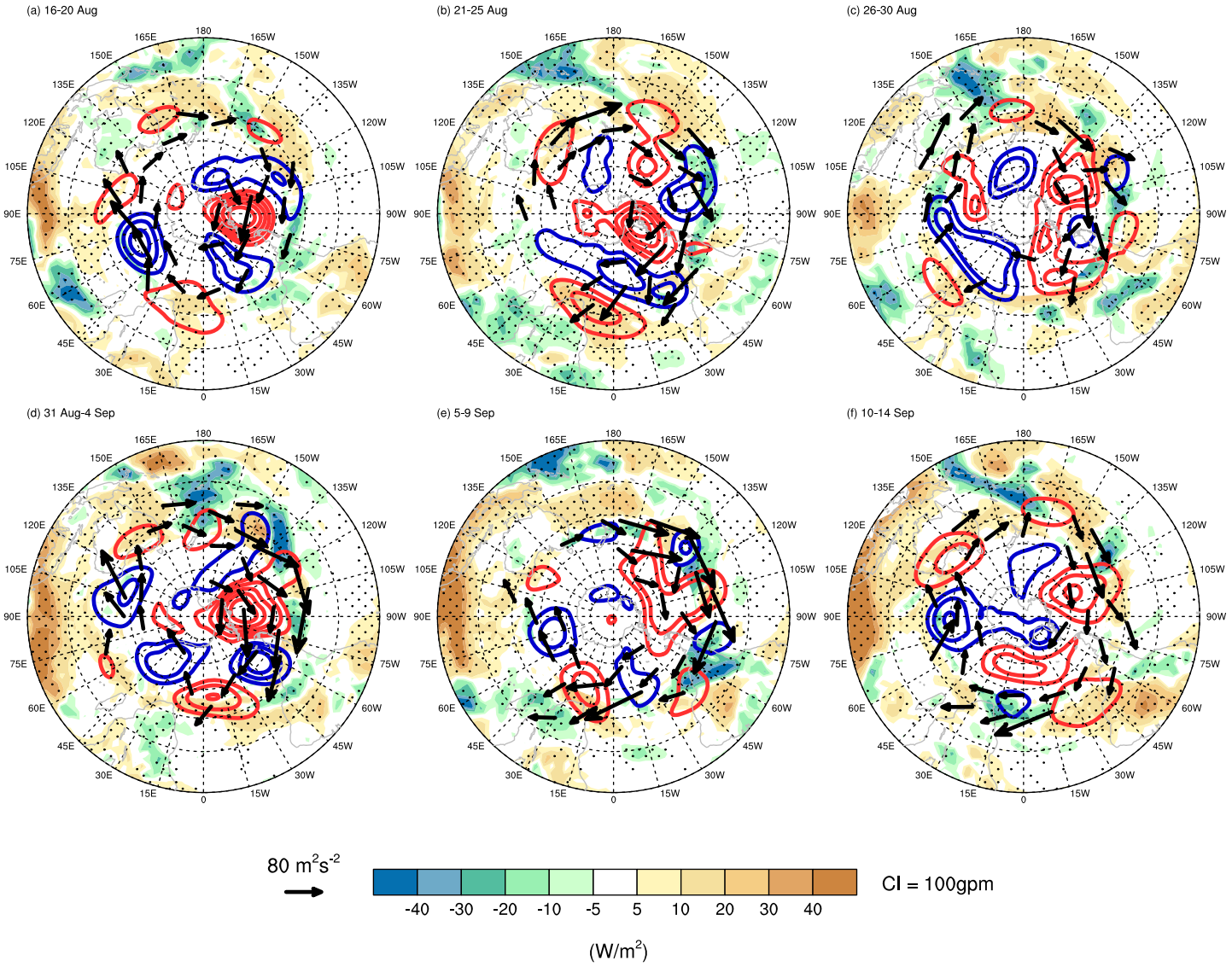

Figure 3. Five-day averaged OLR anomalies (shading, SI = 10 W/m^2), 250-hPa geopotential height anomalies (contour, CI = 100 gpm) and the associated horizontal component of Plumb flux (vector) during the same periods as those in Figure 2. Zero contours are omitted. Blue and red contours denote negative and positive values, respectively. Values exceeding the 99% or 1% percentile estimated from 1,000 bootstrapped samples on each calendar day during 1979–2018 are marked as black dots for the OLR and thick contours for geopotential height anomalies.

train and the resultant eddy heat flux of WN1 decayed (Figure 1f), and a second convection centered around (30°S, 120°W) emerged and amplified over the eastern South Pacific (Figures 3d–3f). The latter reinforced the Rossby wave train again from approximately 10–19 September (Figures 3e and 3f) and explained the temporary recovery of the eddy heat flux around 15 September (Figures 1e–1h). These results suggest that the convection over the Pacific accounts for the persistence and amplification of both the PSA-like Rossby wave train and the eddy heat flux of WN1, thereby contributing substantially to the occurrence of the SSW. Nishii and Nakamura (2004) also found that the 2002 major SSW was linked to anomalous convection to the east of Australia. The hypothesis that centers of Pacific convection may contribute to Antarctic SSW formation warrants future investigation.

Besides the favorable wave forcing from the troposphere, the variability within the stratosphere may also contribute to the occurrence of this minor SSW. The stratospheric tropical winds were easterly above and westerly below 20 hPa during the 2019 SSW (Figure S5a). This condition was also seen in the 2002 SSW

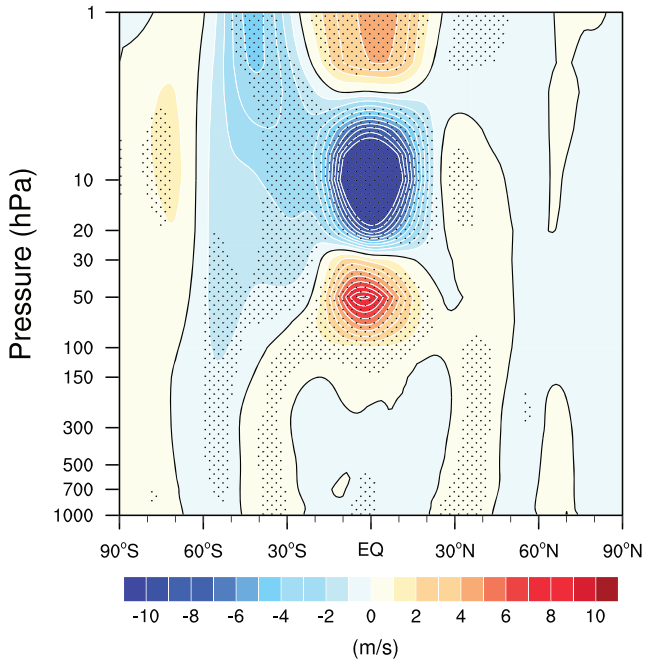

Figure 4. Regression of the August–September averaged zonal mean zonal wind onto the simultaneous QBO index (shading with contour), defined as the 10-hPa FUB zonal wind for the period 1979–2018. A −1 was multiplied to the regression map for visual purposes. Thick black contours denote zero values, and black dots indicate the 90% confidence level based on a two-tailed Student's *t*-test.

and another minor SSW occurred in 1988 (Figures S5b and S5c), and it implies a potential role of the quasi-biennial oscillation (QBO) in facilitating Antarctic SSWs (Gray et al., 2005; Shen et al., 2020). To examine this possibility, an August–September mean QBO index was constructed with the 10-hPa equatorial zonal wind data from the Free University of Berlin (FUB) and regressed onto the simultaneous zonal mean zonal wind (Figure 4). The 10-hPa level, not the commonly used 50-hPa level, was employed because the Holton-Tan relationship (Holton & Tan, 1980) in the Southern Hemisphere is best represented with a zonal wind index in the middle and upper stratosphere (Anstey & Shepherd, 2014; Baldwin & Dunkerton, 1998; Yamashita et al., 2018). Figure 4 shows that the stratospheric circumpolar westerly jet in the Southern Hemisphere weakens significantly when the 10-hPa QBO is in its easterly phase, a phenomenon that was not observed in the seasonal mean fields (Hitchman & Huesmann, 2009). The QBO-related 10-hPa easterlies can result in a strong horizontal wind shear and steep PV gradients in the subtropics, thereby hindering the propagation of planetary waves toward the equator in the stratosphere (Gray et al., 2005). As a result, the Antarctic stratospheric polar vortex is weakened by the deceleration effect of the planetary waves (Gray et al., 2005). Nevertheless, the timescale of the QBO is much longer than the SSW, and the easterly of QBO has persisted for months before the SSW (Figure S5a). Hence, the easterly phase of the QBO in 2019 was not the immediate cause of the SSW in September 2019. In contrast, it facilitated a weak stratospheric polar vortex that is easier to disturb and provided favorable stratospheric conditions for the occurrence of the SSW.

4. Summary and Discussion

This study reveals the possible mechanism underpinning a minor SSW occurring in the Southern Hemisphere during September 2019. The occurrence of this SSW is attributed to the strongest and most persistent upward propagating WN1 from the troposphere since 1979, with almost equal contributions from the instantaneous anomalous WN1 and the linear constructive interference between the anomalous and climatological WN1. The persistence and strength of the anomalous WN1 arose from a long-lived midlatitude Rossby wave train that projected well onto the anomalous WN1, and was sustained by successive anomalous convection to the east of Australia and over the eastern South Pacific. In addition to the tropospheric wave forcing, the upper stratospheric QBO provided favorable stratospheric background conditions for the occurrence of the SSW. Finally, the circulations leading to the 2019 SSW show some similarities with the 2002 major SSW, including anomalous convection over the South Pacific and the descending easterly phase of QBO, indicating some possible precursors of Antarctic SSWs.

A remaining question is what caused the convection that sustained the WN1. A near-record positive Indian Ocean Dipole (IOD) occurred in 2019 and facilitated the occurrence of this SSW (Rao et al., 2020). However, it is unlikely the immediate cause of the convection and thereby the SSW because the subseasonal variations of the IOD index were weak before the SSW (Figure S6). It suggests that the role of the IOD is more likely to set a favored background circulation other than to excite the SSW. The possible role of the Madden-Julian Oscillation (MJO) was also examined. The observed convection does not project well onto the MJO pattern (not shown). Therefore, the convection concerned is more likely a random incident.

It is curious that such vigorous WN1 activity did not lead to a major SSW in 2019. The reason may be due to the absence of other WNs propagating into the stratosphere (Figure 1f–1h, McIntyre, 1982), in contrast to the 2002 major SSW that both WN1 and WN2 contributed. On the one hand, this absence may be attributed to the weak source of the tropospheric WN2. On the other hand, it may also be attributed to the suppressed upward-propagation of WN2 by a strong polar night jet (Charney & Drazin, 1961) because the occurrence of the 2019 SSW is nearer to the peak of austral winter than the 2002 major SSW. Even if the wave energy

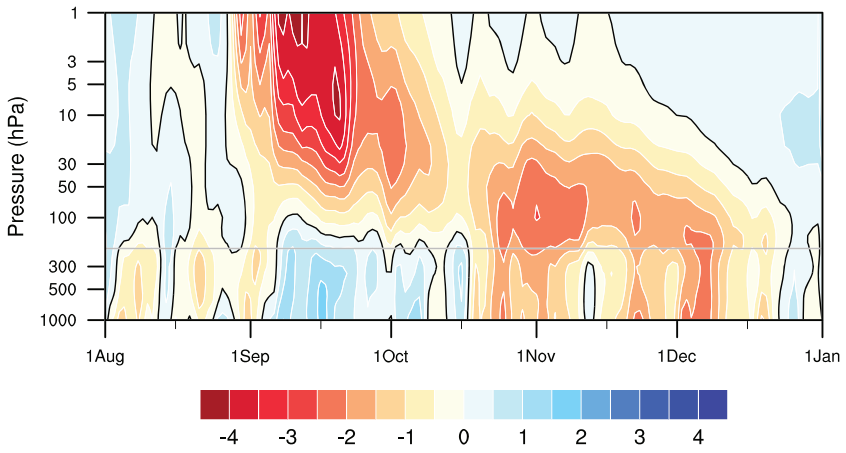

Figure 5. Time-height development of the normalized daily SAM index (shading with contour) from 1 August 2019 to 1 January 2020. Thick black contours indicate zero values. The gray horizontal line indicates the approximate boundary between the troposphere and the stratosphere.

entering the stratosphere were the same in 2002 and 2019, the wave forcing has more work to do in disrupting the stronger early-season vortex in 2019.

Even though the SSW in 2019 is a minor one, its impacts on the climate may be significant. Firstly, the SSW contributed to the smallest Antarctic ozone hole on record (Hu, 2020; Shen et al., 2020; WMO, 2019). Secondly, the negative phase of the SAM associated with the 2019 SSW descended into the troposphere and persisted until the end of 2019 (Figure 5). The associated November–December mean Antarctic Oscillation index was the lowest on record (Figure S7). The resultant tropospheric circulation facilitated anomalous hot and dry conditions over eastern Australia (Figure S8) and increased the risk of wildfires (Lim et al., 2019). It is reported that eastern Australia suffered from unprecedented bushfires since November 2019 (Phillips & Nogrady, 2020). Tens of thousands of indigenous wild animals were killed, and their habitats were destroyed. Our results suggest that the SSW-induced hot and dry conditions likely favored fire development. Nevertheless, other factors, such as the positive IOD, may also contribute. A thorough study is needed to quantify their relative contributions in the future.

Data Availability Statement

The JRA-55 data are available from https://jra.kishou.go.jp/JRA-55/index_en.html.

Acknowledgments

We thank the five anonymous reviewers and the editor for their constructive comments and suggestions that led to significant improvement in the paper. X.S. and L.W. are supported by the National Key R&D Program of China (2018YFC1506003) and the National Natural Science Foundation of China (41925020 and 41721004). S.O. is supported by the Natural Environment Research Council (NE/P006779/1 and NE/N018001/1). The study is an outflow of the Belmont-Forum/JPI-Climate GOTHAM summer school held in Beijing 9–13 September 2019. The authors gratefully acknowledge the tireless workshop support of Prof. Bo Wu.

References

Andrews, D. G., Holton, J. R., & Leovy, C. B. (1987). *Middle atmosphere dynamics*. San Diego: Academic Press Inc.

Anstey, J. A., & Shepherd, T. G. (2014). High-latitude influence of the quasi-biennial oscillation. *Quarterly Journal of the Royal Meteorological Society*, *140*(678), 1–21. https://doi.org/10.1002/qj.2132

Baldwin, M., Hirooka, T., O'Neill, A., Yoden, S., Charlton, A. J., Hio, Y., & Yoden, S. (2003). Major stratospheric warming in the Southern Hemisphere in 2002: Dynamical aspects of the ozone hole split. *SPARC Newsletter*, *20*, 24–26.

Baldwin, M. P., & Dunkerton, T. J. (1998). Quasi-biennial modulation of the southern hemisphere stratospheric polar vortex. *Geophysical Research Letters*, *25*(17), 3343–3346. https://doi.org/10.1029/98GL02445

Charney, J. G., & Drazin, P. G. (1961). Propagation of planetary-scale disturbances from lower into upper atmosphere. *Journal of Geophysical Research*, *66*(1), 83–109. https://doi.org/10.1029/JZ066i001p00083

de la Cámara, A., Birner, T., & Albers, J. R. (2019). Are sudden stratospheric warmings preceded by anomalous tropospheric wave activity? *Journal of Climate*, *32*(21), 7173–7189. https://doi.org/10.1175/JCLI-D-19-0269.1

Gray, L., Norton, W., Pascoe, C., & Charlton, A. (2005). A possible influence of equatorial winds on the September 2002 Southern Hemisphere sudden warming event. *Journal of the Atmospheric Sciences*, *62*(3), 651–667. https://doi.org/10.1175/JAS-3339.1

Hitchman, M. H., & Huesmann, A. S. (2009). Seasonal influence of the quasi-biennial oscillation on stratospheric jets and Rossby wave breaking. *Journal of the Atmospheric Sciences*, *66*(4), 935–946. https://doi.org/10.1175/2008JAS2631.1

Holton, J. R., & Tan, H. C. (1980). The influence of the equatorial quasi-biennial oscillation on the global circulation at 50 mb. *Journal of the Atmospheric Sciences*, *37*, 2200–2208. https://doi.org/10.1175/1520-0469(1980)037<2200:TIOTEQ>2.0.CO;2

Hu, Y. (2020). The very unusual polar stratosphere in 2019–2020. *Science Bulletin*. https://doi.org/10.1016/j.scib.2020.07.011

Kobayashi, S., Ota, Y., Harada, Y., Ebita, A., Moriya, M., Onoda, H., et al. (2015). The JRA-55 reanalysis: General specifications and basic characteristics. *Journal of the Meteorological Society of Japan*, *93*(1), 5–48. https://doi.org/10.2151/jmsj.2015-001

Liebmann, B., & Smith, C. A. (1996). Description of a complete (interpolated) outgoing longwave radiation dataset. *Bulletin of the American Meteorological Society*, *77*, 1275–1277.

Lim, E.-P., Hendon, H. H., Boschat, G., Hudson, D., Thompson, D. W. J., Dowdy, A. J., & Arblaster, J. M. (2019). Australian hot and dry extremes induced by weakenings of the stratospheric polar vortex. *Nature Geoscience*, *12*(11), 896–901. https://doi.org/10.1038/s41561-019-0456-x

Matsuno, T. (1971). A dynamical model of stratospheric sudden warming. *Journal of the Atmospheric Sciences*, *28*(8), 1479–1494. https://doi.org/10.1175/1520-0469(1971)028<1479:ADMOTS>2.0.CO;2

McIntyre, M. E. (1982). How well do we understand the dynamics of stratospheric warmings. *Journal of the Meteorological Society of Japan*, *60*(1), 37–65. https://doi.org/10.2151/jmsj1965.60.1_37

Mo, K. C., & Higgins, R. W. (1998). The Pacific-South American modes and tropical convection during the Southern Hemisphere winter. *Monthly Weather Review*, *126*(6), 1581–1596. https://doi.org/10.1175/1520-0493(1998)126<1581:TPSAMA>2.0.CO;2

Newman, P. A., & Nash, E. R. (2005). The unusual Southern Hemisphere stratosphere winter of 2002. *Journal of the Atmospheric Sciences*, *62*(3), 614–628. https://doi.org/10.1175/JAS-3323.1

Nie, Y., Zhang, Y., Yang, X. Q., & Chen, G. (2013). Baroclinic anomalies associated with the Southern Hemisphere Annular Mode: Roles of synoptic and low-frequency eddies. *Geophysical Research Letters*, *40*, 2361–2366. https://doi.org/10.1002/grl.50396

Nishii, K., & Nakamura, H. (2004). Tropospheric influence on the diminished Antarctic ozone hole in September 2002. *Geophysical Research Letters*, *31*, L16103. https://doi.org/10.1029/2004GL019532

Nishii, K., Nakamura, H., & Miyasaka, T. (2009). Modulations in the planetary wave field induced by upward-propagating Rossby wave packets prior to stratospheric sudden warming events: A case-study. *Quarterly Journal of the Royal Meteorological Society*, *135*(638), 39–52. https://doi.org/10.1002/qj.359

Nishii, K., Nakamura, H., & Orsolini, Y. J. (2011). Geographical dependence observed in blocking high influence on the stratospheric variability through enhancement and suppression of upward planetary-wave propagation. *Journal of Climate*, *24*(24), 6408–6423. http://doi.org/10.1175/JCLI-D-10-05021.1

Phillips, N., & Nogrady, B. (2020). The race to decipher how climate change influenced Australia's record fires. *Nature*, *577*(7792), 610–612. http://doi.org/10.1038/d41586-020-00173-7

Plumb, R. A. (1985). On the 3-dimensional propagation of stationary waves. *Journal of the Atmospheric Sciences*, *42*(3), 217–229. http://doi.org/10.1175/1520-0469(1985)042<0217:OTTDPO>2.0.CO;2

Polvani, L. M., & Waugh, D. W. (2004). Upward wave activity flux as a precursor to extreme stratospheric events and subsequent anomalous surface weather regimes. *Journal of Climate*, *17*, 3548–3554. http://doi.org/10.1175/1520-0442(2004)017<3548:UWAFAA>2.0.CO;2

Rao, J., Garfinkel, C. I., White, I. P., & Schwartz, C. (2020). The Southern Hemisphere minor sudden stratospheric warming in September 2019 and its predictions in S2S models. *Journal of Geophysical Research: Atmospheres*, *125*, e2020JD032723. https://doi.org/10.1029/2020JD032723

Sardeshmukh, P. D., & Hoskins, B. J. (1988). The generation of global rotational flow by steady idealized tropical divergence. *Journal of the Atmospheric Sciences*, *45*, 1228–1251. https://doi.org/10.1175/1520-0469(1988)045<1228:TGOGRF>2.0.CO;2

Shen, X., Wang, L., & Osprey, S. (2020). The Southern Hemisphere sudden stratospheric warming of September 2019. *Science Bulletin*, *65*(21), 1800–1802. https://doi.org/10.1016/j.scib.2020.06.028

Sjoberg, J. P., & Birner, T. (2012). Transient tropospheric forcing of sudden stratospheric warmings. *Journal of the Atmospheric Sciences*, *69*(11), 3420–3432. https://doi.org/10.1175/JAS-D-11-0195.1

Smith, K. L., & Kushner, P. J. (2012). Linear interference and the initiation of extratropical stratosphere-troposphere interactions. *Journal of Geophysical Research*, *117*, D13107. https://doi.org/10.1029/2012JD017587

Thompson, D. W. J., Baldwin, M. P., & Solomon, S. (2005). Stratosphere-troposphere coupling in the Southern Hemisphere. *Journal of the Atmospheric Sciences*, *62*(3), 708–715. https://doi.org/10.1175/JAS-3321.1

Waugh, D. W., & Polvani, L. M. (2010). Stratospheric polar vortices. In L. M. Polvani, et al. (Eds.), *The stratosphere: Dynamics, transport, and chemistry* (pp. 43–57). Washington, DC: American Geophysical Union. https://doi.org/10.1029/GM190

White, I., Garfinkel, C. I., Gerber, E. P., Jucker, M., Aquila, V., & Oman, L. D. (2019). The downward influence of sudden stratospheric warmings: Association with tropospheric precursors. *Journal of Climate*, *32*(1), 85–108. https://doi.org/10.1175/JCLI-D-18-0053.1

World Meteorology Organization (2019). Antarctic ozone hole is smallest on record. Accessed October 2019 at https://public.wmo.int/en/media/news/antarctic-ozone-hole-smallest-record

Xiao, B., Zhang, Y., Chen, G., & Yang, X. Q. (2016). On the role of extratropical air-sea interaction in the persistence of the Southern Annular Mode. *Geophysical Research Letters*, *43*, 8806–8814. https://doi.org/10.1002/2016GL070255

Yamashita, Y., Naoe, H., Inoue, M., & Takahashi, M. (2018). Response of the Southern Hemisphere atmosphere to the stratospheric equatorial quasi-biennial oscillation (QBO) from winter to early summer. *Journal of the Meteorological Society of Japan*, *96*(6), 587–600. https://doi.org/10.2151/jmsj.2018-057

Yamazaki, Y., Matthias, V., Miyoshi, Y., Stolle, C., Siddiqui, T., Kervalishvili, G., et al. (2020). September 2019 Antarctic sudden stratospheric warming: Quasi-6-day wave burst and ionospheric effects. *Geophysical Research Letters*, *47*, e2019GL086577. https://doi.org/10.1029/2019GL086577